Scientific Research and Essays Vol. 6(29), pp. 6082-6094, 30 November, 2011
Available online at http://www.academicjournals.org/SRE
DOI: 10.5897/SRE11.727
ISSN 1992-2248 ©2011 Academic Journals

Full Length Research Paper

Obtaining soil stiffness using WAK test and numerical methods

Mansour Parvizi and Hossein Sharif*

[1]Geotechnical Group, School of Engineering, University of Yasuj, Iran.
[2]Faculty of Technology, University of Portsmouth, PO1 3HE, U. K.

Accepted 31 October, 2011

A study has been undertaken at musicale in the laboratory to simulate the densification of a sandy soil bed by dynamic compaction. This was achieved by allowing a tamper mass of 875 gm to fall through 100 mm onto a stiff aluminium target having a mass of 268 gm and a diameter of 100 mm. Since the frequencies generated by this process are very low, the dynamic stiffness derived approximately the static value derived from a monotonic load test (static load test). In total, 9 different experiments were carried out; three impact tests and six static load tests. Consequently, a number of numerical models were constructed to simulate impact load and static load tests. Overall, soil stiffness was obtained using six different methods. Analysis of the results demonstrates that the soil stiffness obtained in the impact test by Fast Fourier Transform analysis (experimental and numerical) and the stiffness obtained through static load test (experimental and numerical) all agreed reasonably well. The conclusion derived from this study confirms the reliability of numerical methods for obtaining sandy soil stiffness, which are significantly more economical as compared to experimental methods. Furthermore, this study can now be extended through development of a numerical model test in flight (multi- g) in the centrifuge to validate (static) soil stiffness computed by the WAK test.

Key words: WAK test, numerical methods, soil stiffness, centrifuge modelling, dynamic compaction, soil improvement, linear systems, impact load testing.

INTRODUCTION

Dynamic compaction is defined as the densification of soil deposits by means of repeatedly dropping a heavy weight onto the ground surface (Figure 1) (Chow et al., 1992, 1994). Historically, this has been achieved by dropping a weight of between 5 and 30 tones through a height of between 10 and 40 metres onto the ground surface in a predetermined pattern over the area to be treated (Merrifield et al. 1998, 2004; Parvizi, 2006).

In general, the ultimate goals of dynamic compaction are to increase bearing capacity and decrease total and differential settlements within a specified depth of improvement.

The degree of soil improvement and the extent to which the improvement penetrates the soil bed depend on a number of factors (Merrifield et al., 1998):

1. The nature of the soil, including soil classification, degree of saturation, initial relative density, permeability and drainage path length.
2 .Mass of the drop weight or pounder, distance of fall and energy imparted to the soil per impact.
3. Number of impacts per location and spacing of the impact locations over the area being treated.

The estimate of the enhancement of soil behaviour in terms of increased soil stiffness (K) and depth of improvement (D) has, to date, been largely empirical (Charles and Watts, 1982; Lukas, 1980; Menard and Broise, 1975).

*Corresponding author. E-mail: Hossein.Sharif@port.ac.uk.

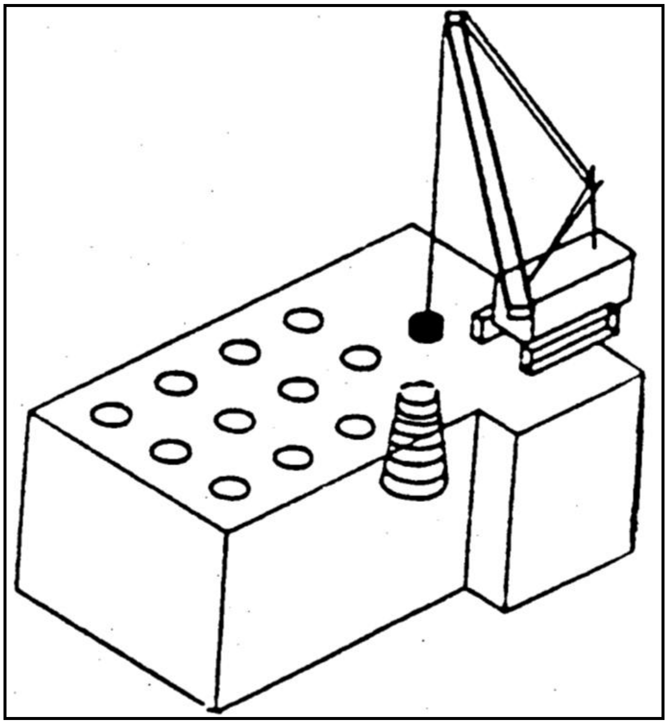

Figure 1. Dynamic compaction (Lukas, 1995).

In an attempt to provide a rapid, economical and efficient method of soil improvements in situations where traditional dynamic compaction is infeasible, expensive and/or time-consuming, compaction is achieved by imparting a significantly lighter load through a shorter height compared with the traditional high-energy compaction process. This technique is often referred to Low-Energy Dynamic Compaction (LEDC); involving typically a mass of seven tonnes falling through a height of 2 metres on to the target surface (Parvizi 2009; Parvizi and Merrifield, 2002). This method has been specially developed for the rapid improvement of a foundation soil to a modest depth of up to 3 metres (Watts and Charles 1993). It is termed 'low energy' because the energy input per blow is low compared with that imparted by traditional dynamic compaction techniques (Parvizi, 2009).

The apparatus for low-energy dynamic compaction, designed and built by BSP International Foundation Ltd, was originally targeted for the rapid repair of bomb damaged airfield runways. However, the compactor was later adapted for civil engineering purposes and is referred to be an ideal method of treating various types of fill and coarse-grained materials (Allen, 1996, Parvizi, 2009).

An important issue in LEDC is the establishment of suitable methods of measuring soil stiffness, which are necessary in gaining the confidence of the engineering team in utilising this compaction method. In general, a suitable method for measuring soil stiffness for LEDC has to be: reliable, rapid and economical. Such methods can be broadly categorised into two main groups: WAK test methods and SLT methods (Parvizi, 1999). So far, there has been limited research on these methods; researchers usually provide their analysis of LEDC based on one or two of these methods. This research notably presents a series of experiments and numerical tests on LEDC less than 1 g centrifuge and evaluates the results based on six distinct methods of measuring soil stiffness. Additionally, this paper also highlights the use of numerical methods in measuring soil stiffness under LEDC. Consequently, this study derives a number of conclusions regarding each of these methods and provides an analysis of the improvement achieved in soil stiffness using low energy dynamic compaction.

MATERIALS AND METHODS

Model preparation

A soil bed of fine Mersey River sand (D50 = 0.2 mm, Coefficient of uniformity, Cu = 1.5) was constructed by dry pluviation into a rigid model container having sides of 580 mm and a depth of 460 mm. The model comprised a uniform bed of loose sand having a relative density of about 35.5 ± 2% (Table 1). A stiff aluminium target (diameter = 100 mm), instrumented with an accelerometer active in the vertical axis, was placed on the sand surface at the location of impact. Impact was applied to this target by a pounder instrumented with a dynamic load cell. High frequency signals were buffered by covering the target with a thin rubber sheet (Figure 2) (Parvizi and Merrifield, 2000).

WAK test analysis

An adoption of the Wave Activation Stiffness (*K*) or WAK Test, a non-destructive test originally designed to assess the static stiffness of soil beneath a rigid footing (Figure 3) (Briaud and Lepert 1990), developed further by Allen (Allen 1996, Allen et al. 1994), was used to predict the increase in static stiffness of the target/soil system, the mass of the vibrated, system damping coefficient and the depth of improvement due to the dynamic compaction (Parvizi and Merrifield, 2002).

The test was performed by applying a blow of known magnitude to the rigid target or footing near its centre. This impact caused the footing and soil immediately beneath it to vibrate. The velocity signal of this vibration, derived from the accelerometer data, and the force input signal from the drop weight were used to calculate the frequency response function by taking the ratio of the Fourier transform of the response signal, *v(t)*, to the Fourier transform of the input signal, *F(t)*. This transfer function is a measure of the mobility, *v/F*, of the system.

This analysis, which assumes a single degree of freedom system to model the footing/soil behaviour, is used to determine the internal damping of the system, *C*, the stiffness of the soil underlying the footing, *K*, and the theoretical mass of soil and footing, *M*, which contributes to the behaviour of the system (Figure 4) (Briaud and Lepert, 1990; Maxwell and Briaud, 1983; Tschirart and Briaud, 1992). The equation of motion of the system according to the model by using Newton's second law is (Clough and Penzien, 1975; Lysmer and Richart ,1966; Rao ,1990):

Table 1. Initial relative density (D_r) for impact load, numerical and static load tests.

Test	Initial relative density Dr (%)	Type of Test Experimental	Type of Test numerical	Type of tests (after & before) impact (experimental)	Type of test numerical
1	37.6	Impact	Impact	SLT	SLT
2	33.5	Impact	Impact	SLT	SLT
3	35.2	Impact	Impact	SLT	SLT

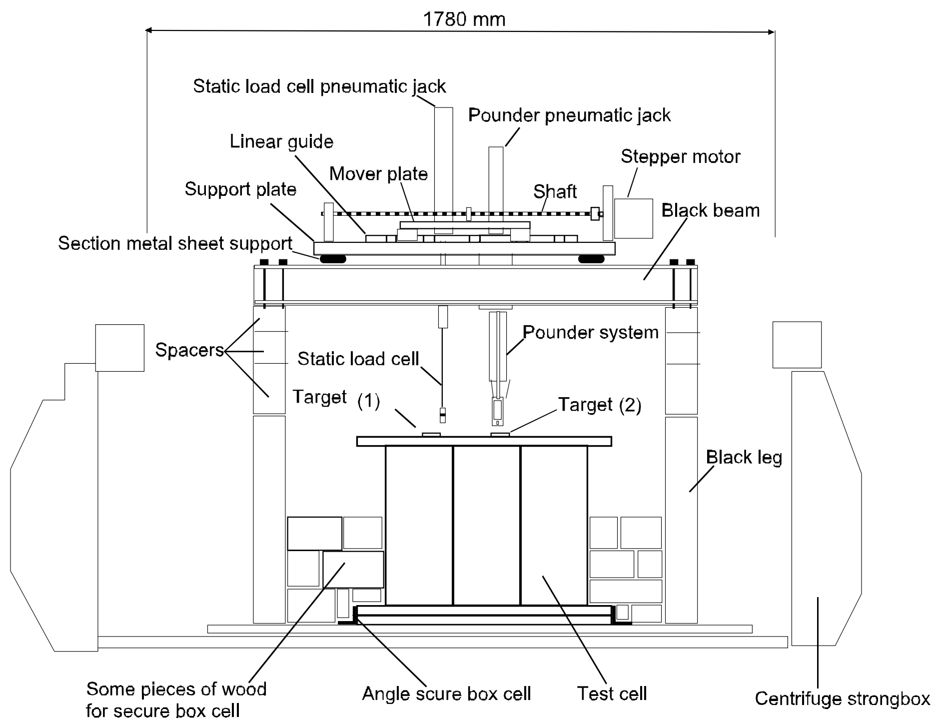

Figure 2. Dynamic compaction test set-up.

$$F_1 + F_2 + F_3 = F(t) \quad (1)$$

Where; F_1 = Force due to mass (*M*); F_2 = Force due to damping (*C*); F_3 = Force due to spring (*K*).

Since system is assumed to be linear, the law of superposition can be applied:

$$F_1 = M\ddot{x} \quad (2)$$

$$F_2 = C\dot{x} \quad (3)$$

$$F_3 = Kx \quad (4)$$

Substitute F_1, F_2 and F_3 in equation 1, gives:

$$M\ddot{x} + C\dot{x} + Kx = F(t) \quad (5)$$

Where; *M*: the mass of weight plus added mass of vibrating soil; *C*: the damping coefficient; *K*: the stiffness of the vibrating soil; *x*: the vertical displacement of the footing subjected to the dynamic force $F(t)$.

By assuming that the system is excited harmonically, the force applied is sinusoidal and the dynamic load equal to:

$$F(t) = F_0 e^{J\omega t} \quad (6)$$

Or;

$$F(t) = F_0 \cos \omega t + F_0 J \sin \omega t \quad (7)$$

$F(t)$ has two parts, the first part is real part and the second part is imaginary. Since the system is modelled as linear, equation 5 may be solved by superposition:

$$x(t) = x_1(t) + x_2(t) \quad (8)$$

Where; $x(t)$: the solution to the equation; $x_1(t)$: the general solution

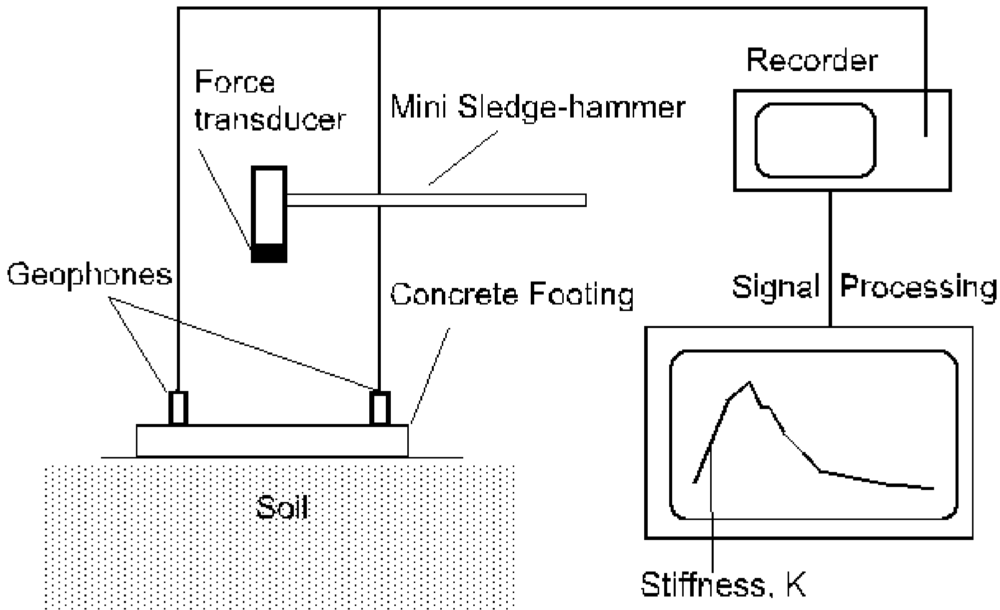

Figure 3. Schematic diagram of the WAK test set-up.

for equation 5 with the right-hand side equal to zero or (complementary function); $x_2(t)$: the particular integral(solution). Before solving equation 5, it is appropriate to define some parameters and how they are related to the equation of motion. It is also useful to present solutions of this equation for particular cases. Finally the general solution for equation 5 is:

$$x_1(t) = e^{-r\omega_n}\left[A\sin\omega_d t + B\cos\omega_d t\right] \tag{9}$$

In order to find $x_2(t)$, in the equation of motion (equation 5), it is assumed that the system is excited harmonically, that is, The force applied is sinusoidal in shape, $F(t)$ can be represented as $F_0 e^{J\omega t}$. The equation of motion then becomes:

$$M\ddot{x} + C\dot{x} + Kx = F_0 e^{J\omega t} \tag{10}$$

This assumes that the impact signal is infinite in length, which obviously, is not the case. However, a finite phenomenon can be represented by an infinite sum of properly weighted sine and cosine functions.

$$x = Ve^{J\omega t} \tag{11}$$

$$\dot{x} = J\omega Ve^{J\omega t} \tag{12}$$

$$\ddot{x} = -\omega^2 Ve^{J\omega t} \tag{13}$$

Substituting the equations 11, 12, 13 in the equation 10 gives:

$$M\left(-\omega^2 Ae^{J\omega t}\right) + C\left(J\omega Ae^{J\omega t}\right) + K\left(Ae^{J\omega t}\right) \equiv F_0 e^{J\omega t} \tag{14}$$

$$\left(-M\omega^2 + JC\omega + K\right)V \equiv F_0 \tag{15}$$

Therefore;

$$V = \frac{F_0}{\left(-M\omega^2 + CJ\omega + K\right)} \tag{16}$$

Multiplying the numerator and denominator on the right side of equation 16, $\left[\left(K - M\omega^2\right) - JC\omega\right]$ and separating the real part and imaginary part, we get:

$$V = F_0\left[\frac{-M\omega^2 + K}{\left(K - M\omega^2\right)^2 + C^2\omega^2} - \frac{JC\omega}{\left(K - M\omega^2\right)^2 + C^2\omega^2}\right] \tag{17}$$

Using the relation, $V = a \pm Jb = Ae^{\pm J\beta}$ where $A = \sqrt{a^2 + b^2}$ and z
Then equation 17 can be expressed as:

$$A = \sqrt{\frac{F_0^{\,2}\left(K - M\omega^2\right)^2}{\left[\left(K - M\omega^2\right)^2 + C^2\omega^2\right]^2} + \frac{F_0^{\,2}C^2\omega^2}{\left[\left(K - M\omega^2\right)^2 + C^2\omega^2\right]^2}} \tag{18}$$

$$A = \frac{F_0}{\left[\left(K - M\omega^2\right)^2 + C^2\omega^2\right]^{1/2}} \tag{19}$$

$$V = Ae^{-J\beta} \tag{20}$$

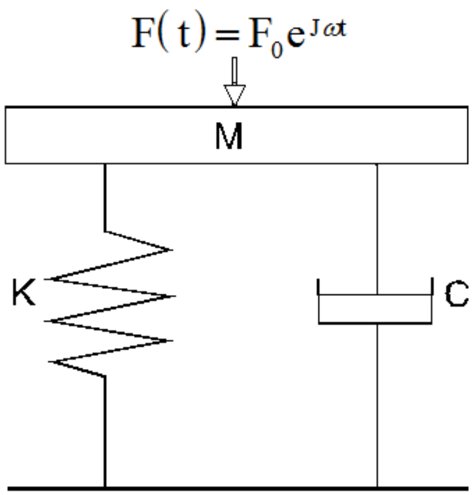

Figure 4. Soil footing model with the single degree of freedom (SDOF).

Substitute *A*, from equation 19, into equation 20 giving:

$$V = \frac{F_0}{\left[\left(K - M\omega^2\right)^2 + C^2\omega^2\right]^{1/2}} e^{-J\beta} \tag{21}$$

$$x_2(t) = Ve^{J\omega t} \tag{22}$$

$$x_2(t) = \frac{F_0}{\left[\left(K - M\omega^2\right)^2 + C^2\omega^2\right]^{1/2}} e^{-J\beta} \times e^{J\omega t} \tag{23}$$

Thus the steady-state solution becomes;

$$x_2(t) = \frac{F_0}{\left[\left(K - M\omega^2\right)^2 + C^2\omega^2\right]^{1/2}} e^{J(\omega t - \beta)} \tag{24}$$

The exponential term in equation 9, will die away after a sufficiently long time, *t*, so the general solution becomes:

$$x_1(t) = 0 \tag{25}$$

Then ;

$$x(t) = x_1(t) \tag{26}$$

$$x(t) = \frac{F_0}{\left[\left(K - M\omega^2\right)^2 + C^2\omega^2\right]^{1/2}} e^{J(\omega t - \beta)} \tag{27}$$

When a harmonic force is applied to a single-degree-of-freedom system, the response of this system is also harmonic after a few moments, then by differentiating equation 27, to give the velocity of the system (footing):

$$v(t) = \frac{F_0\omega}{\left[\left(K - M\omega^2\right)^2 + C^2\omega^2\right]^{1/2}} e^{J\left(\omega t - \beta + 90^0\right)} \tag{28}$$

$$\beta = \tan^{-1}\left(\frac{C\omega}{K - M\omega^2}\right) \tag{29}$$

Differentiating again to obtain the acceleration of the system (footing);

$$a(t) = \frac{F_0\omega^2}{\left[\left(K - M\omega^2\right)^2 + C^2\omega^2\right]^{1/2}} e^{J\left(\omega t - \beta + 180^0\right)} \tag{30}$$

The transfer function or mobility of the system is the ratio between the response (velocity), and the input (force), in terms of circular frequency, ω :

$$\frac{v}{F}(\omega) = \frac{\dfrac{F_0\omega}{\left[\left(K - M\omega^2\right)^2 + C^2\omega^2\right]^{1/2}} e^{J\left(\omega t - \beta + 90^0\right)}}{F_0 e^{J\omega t}} \tag{31}$$

$$\frac{v}{F}(\omega) = \frac{\omega}{\left[\left(K - M\omega^2\right)^2 + C^2\omega^2\right]^{1/2}} e^{J\left(-\beta + 90^0\right)} \tag{32}$$

The transfer function of the system can be calculated as the ratio between the response (acceleration) and the input (force), in terms of circular frequency, ω :

$$\frac{a}{F}(\omega) = \frac{\dfrac{F_0\omega^2}{\left[\left(K - M\omega^2\right)^2 + C^2\omega^2\right]^{1/2}} e^{J\left(\omega t - \beta + 180^0\right)}}{F_0 e^{J\omega t}} \tag{33}$$

$$\frac{a}{F}(\omega) = \frac{\omega^2}{\left[\left(K - M\omega^2\right)^2 + C^2\omega^2\right]^{1/2}} e^{J\left(-\beta + 180^0\right)} \tag{34}$$

Where the acceleration recorded rather than velocity, the mobility function may be found by dividing accelerance, i.e. the transfer function between acceleration and force by the circular frequency, ω :

$$\left|\frac{v}{F}(\omega)\right| = \frac{\left|\dfrac{a}{F}(\omega)\right|}{\omega} \tag{35}$$

Where;

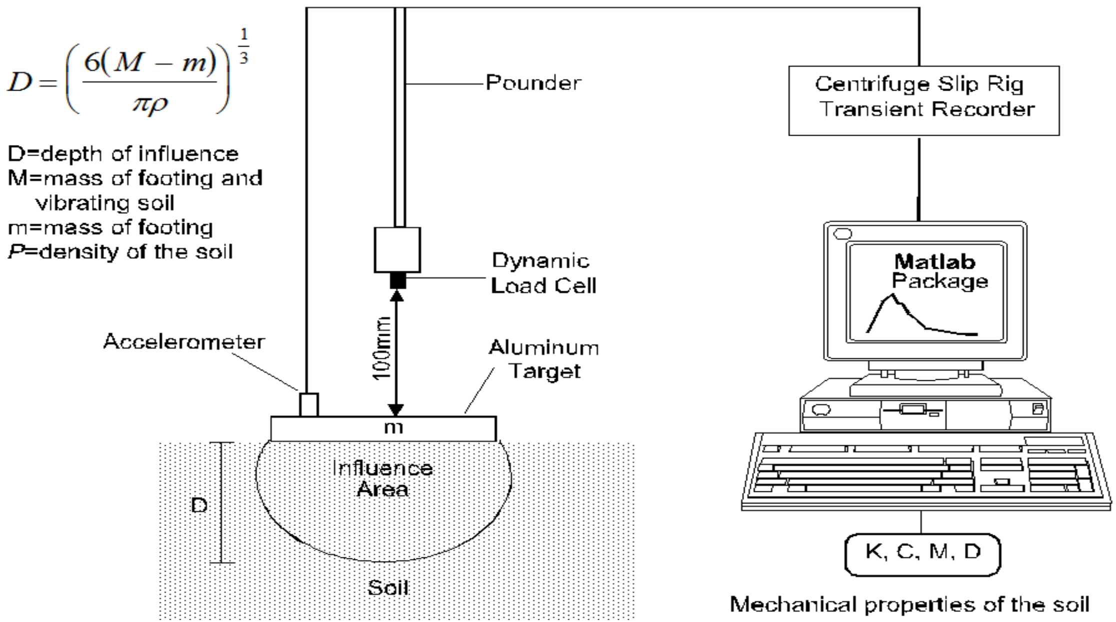

Figure 5. The WAK test diagram for centrifuge modeling.

$\left|\frac{v}{F}(\omega)\right|$ is equal to the real part of the equation 32 and is the absolute value of the transfer function.

$\left|\frac{a}{F}(\omega)\right|$ is the real part of the equation 35 and is the absolute value of the acceleration (response) and force (input).

This method is preferred to that of integrating the acceleration signal to yield velocity since errors of integration are magnified during signal processing. The transfer function has one peak since the system has one degree of freedom.

Measurement by the load cell of the input force, *F*, due to the impact of the falling drop weight and resultant acceleration response of the target measured by an accelerometer placed on the target itself, provided the required output data for the analysis (Figure 5). The stiffness of the soil and drop-weight combined system, the mass and the damping of the system are expressed by expansion of the transfer function, that is,

$$\left|\frac{v}{F}(\omega)\right| = \frac{\omega}{\left[(K - M\omega^2)^2 + C^2\omega^2\right]^{1/2}} \quad (36)$$

Differentiating with respect to frequency and setting to zero gives the relationship between *K*, and *M* at the un-damped natural frequency of the system ω_n, i.e.

$$\frac{1}{\left[(K - M\omega^2)^2 + C^2\omega^2\right]^{1/2}} - \frac{4M^2\omega^4 - 4KM\omega^2 + C^2\omega^2}{2\left[(K - M\omega^2)^2 + C^2\omega^2\right]^{3/2}} = 0 \quad (37)$$

Hence; $\omega = \omega_n = \sqrt{\frac{K}{M}}$ (38)

Substituting equation 38 into equation 37 gives:

$$\left.\left|\frac{v}{F}(\omega)\right|\right|_{\omega=\omega_n} = \frac{1}{C} \quad (39)$$

Investigation of another point on the curve, that is, ω_1 , $\left.\left|\frac{v}{F}(\omega)\right|\right|_{\omega=\omega_2}$ allows the calculation of the mass, *M*, by the solution of equation 1, and *K* by subsequent substitution into equation 38.

$$M = \frac{\sqrt{\frac{\omega_1{}^2}{\left.\left|\frac{v}{F}(\omega)\right|\right|_{\omega=\omega_1}^{2}} - -C^2\omega_1{}^2}}{\left|\omega_n{}^2 - \omega_1{}^2\right|} \quad (40)$$

The theoretical depth of influence (*D*) due to the dynamic loading may be calculated by assuming a volumetric characteristic for the mass of soil contributing to the vibration. This is normally assumed to be truncated-spherical (Figure 5). Since the transient signal is periodic, it is necessary to represent it by means of a discrete Fourier Transform.

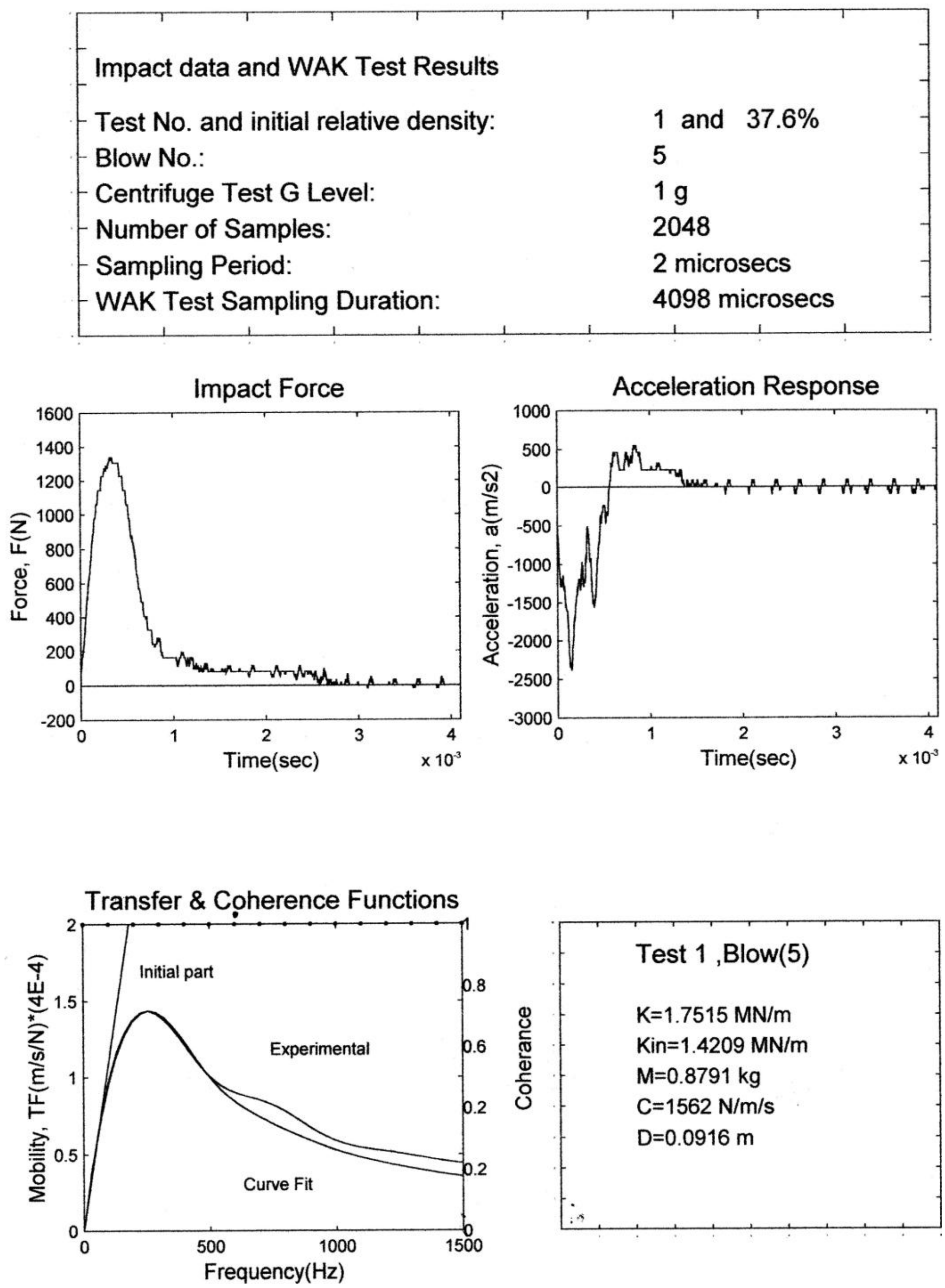

Figure 6. Typical impact data and parameters derived from the WAK Test for blow 5.

Using Matlab, a commercially available signal-processing package, the transfer function derived from the experimental data may be found (Parvizi 1999; Parvizi and Merrifield, 2004).

Likewise the coherence function may be determined to assess the reliability of the data. A value of unity for the coherence function will be returned for a perfect relationship between input (F_ω) and the output (v_ω) signals (Brooke and Wynne, 1988; Gobert and Pak, 1994; Parvizi, 1999). Since the transfer function is inevitably irregular an iterative process of curve fitting was used to determine the best-fit values for *K*, *M* and the damping factor, C (Tschirart and Briaud, 1992). Figure 6 shows typical data (force input, F and accelerations output, a) and derived transfer function for a single blow (blow 5 in a series of blows for test1 with relative density 37.6%). From these data the soil stiffness for blow five is; *K* = 1.7515 MN/m.

Soil stiffness by initial part of transfer function

There is another method to determine soil stiffness (*K*), which is based on transfer function curve. In theory, the slope of the transfer

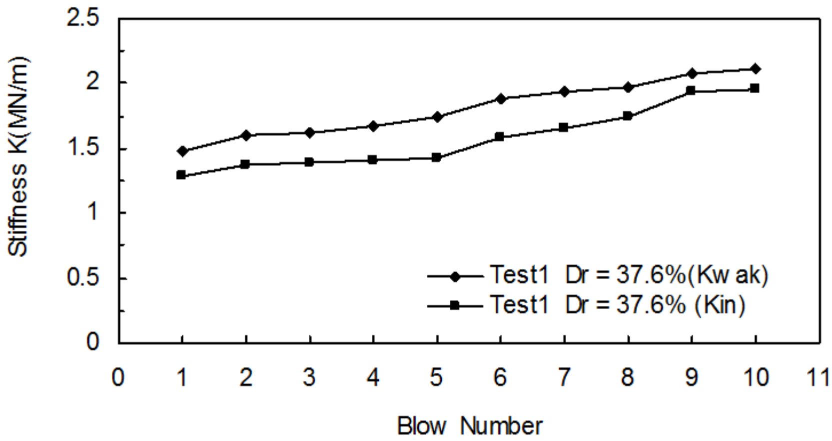

Figure 7. Soil stiffness by WAK test and by initial part of transfer function plot against blow number.

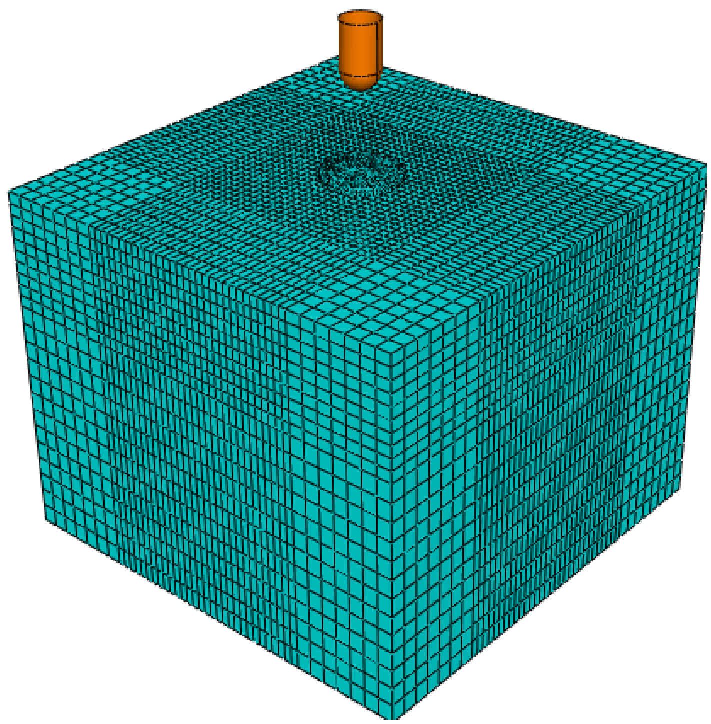

Figure 8. Schematic 3-D mesh for dynamic compaction test.

function at the origin is inversely proportional to stiffness (*K*), (Briaud and Lepert, 1990). Based on this, the following expression can be used to calculate *K*.

$$K_{\mathrm{in}} = \frac{2\pi(\Delta f)}{\left[\Delta\left|\frac{v}{F}(\omega)\right|\right]_{At\ the\ origin}} \quad (42)$$

Based on the expression earlier mentioned, and using the transfer function as presented in Figure 6, the value of K_{in} was obtained. Notably, the value of K_{in} = 1.4209 MN/m obtained via this method was reasonably close to the value of *K* obtained through curve fitting in the transfer function generated by the WAK test. Figure 7 shows the *K* by WAK Test with K_{in} by initial part of transfer function for test1 (Dr = 37.6%).

Numerical WAK test

A 3-D mesh describing the soil bed and the footing system based on WAK Test for the FE analysis was prepared by the ABAQUS software package for dynamic compaction (impact load) test, see Figure 8. A more detailed illustration for this numerical method in a 2-D setting is

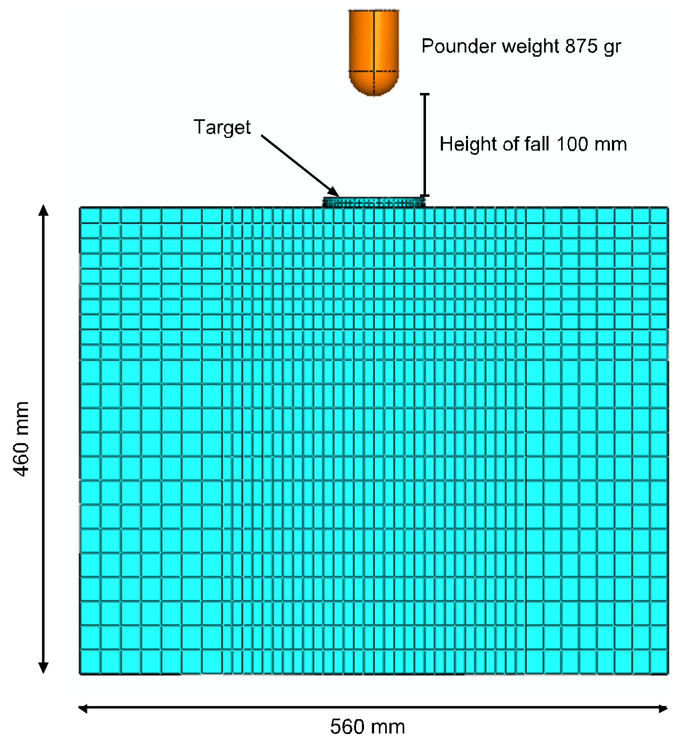

Figure 9. Schematic 2-D mesh for dynamic compaction test.

presented in Figure 9. Figure 10 shows typical data by numerical method (force input, F and accelerations output, a) and the transfer function derived for a single blow. From these data the stiffness for a single blow (Test1 relative density, 37.6%) is: k = 1.638 MN/m, K_{in}= 1.419 MN/m. Figure 11 shows the stiffness obtained using the numerical WAK Test and the initial part of transfer function (K_{in}).

The monotonic load-displacement test (SLT)

In total, three plate load (static load) tests before and after dynamic processes were conducted accompanied with dynamic compaction with the same relatively density (Table 1).

The static load cell was calibrated using a triaxial compression rig in centrifuge laboratory at the University of Manchester (Figure 12).

The test set-up for the compaction process and SLT is presented in Figure 2. As shown there are two identical footings; one footing is used for the static load test (SLT) before dynamic compaction process (Target 1) and the other footing which is situated at least two diameters away from the first one was used for dynamic compaction processes and later for SLT after dynamic compaction (Target 2). The distance between the two footings ensures that the compaction process does not affect the other footing.

The static load tests (SLT) were performed before and after dynamic compaction (Figure 2). An example of the curves obtained is shown in Figure 13. From this curve, the stiffness can be obtained by calculating the slope at the origin.

The data obtained for three static load tests, before and after dynamic compaction processes, are presented in Table 2.

Numerical modelling of the monotonic load-displacement test

A 3-D mesh for FE analysis describing the soil bed and the footing system was developed using the ABAQUS software package and then used for monotonic load test. The monotonic load test was simulated by the application of a series of load steps. Each load step was equal to 10N and for each step the displacement was recorded (Figure 14). It was assumed that within the load range (at low loads magnitudes) the soil behaviour was linear-elastic. The numerical load-displacement curve was plotted which was similar to Figure 13. The stiffness values (before and after dynamic compaction) were then obtained by calculating the slope of the curve at the origin. Based on this method, the numerical stiffness before and after dynamic compaction was 1.191 and 2.062 MN/m respectively (Test1). The value of k derived from the numerical SLT for three tests are presented in Table 3.

RESULTS AND DISCUSSION

In the present research, soil stiffness for dynamic compaction was derived using four experimental and three numerical methods based on WAK test and SLT. The results of the study, as illustrated in Figures 15 and 16, demonstrate soil stiffness values obtained using these methods were reasonably close. Most notably, the results of this research highlight the reliability of numerical methods in modelling dynamic compaction and their potential use in confirming soil stiffness values derived using experimental methods.

Conclusion

In general, numerical methods for obtaining soil stiffness

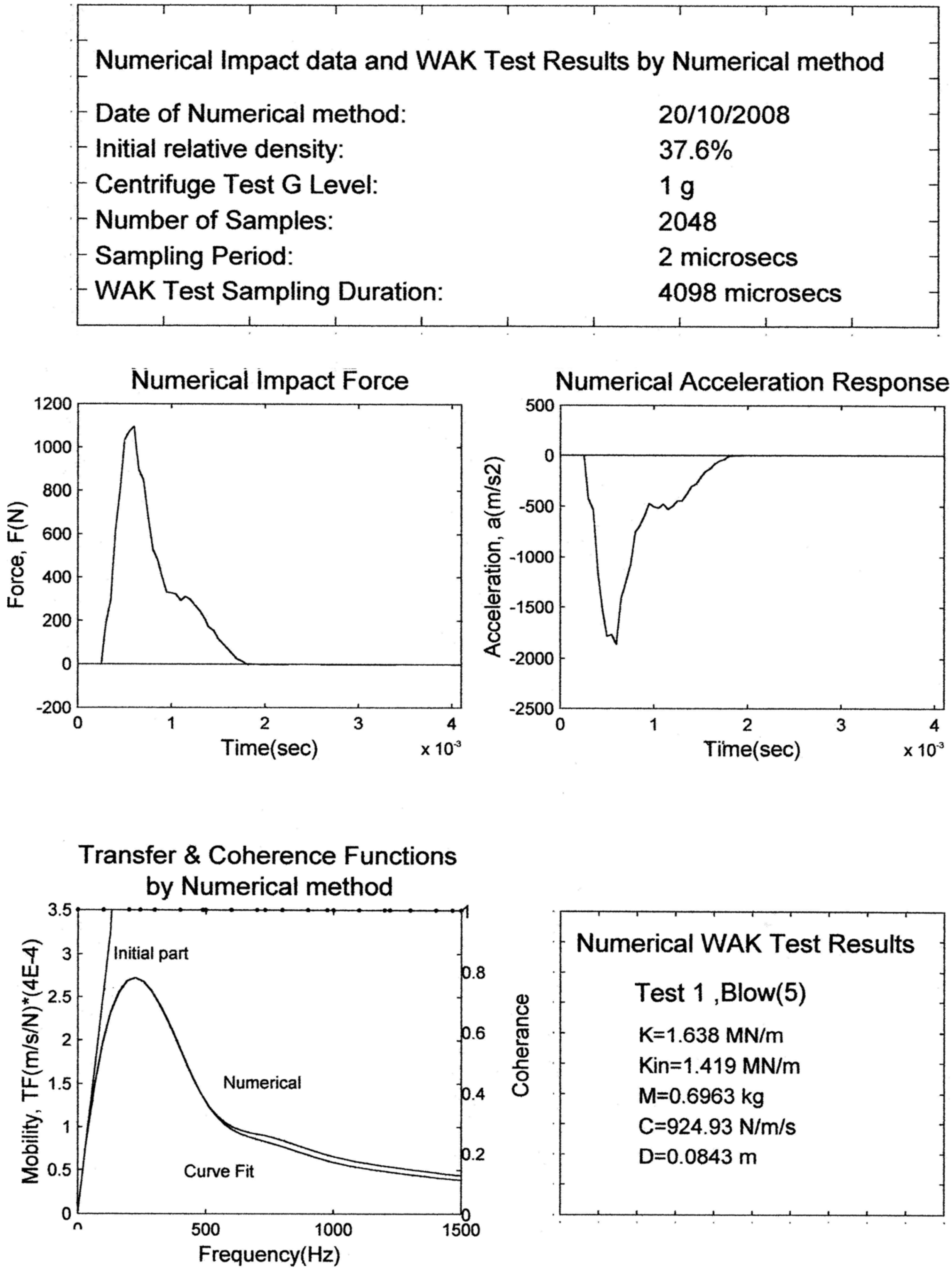

Figure 10. Typical impact data by numerical method based on WAK Test for blow 5.

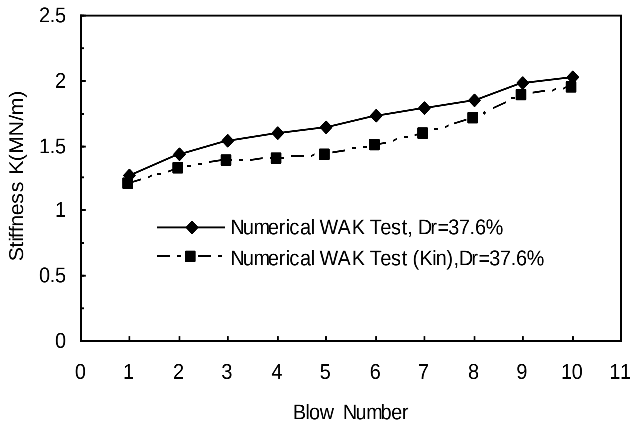

Figure 11. Numerical soil stiffness by WAK test and by initial part of transfer function plot against blow number.

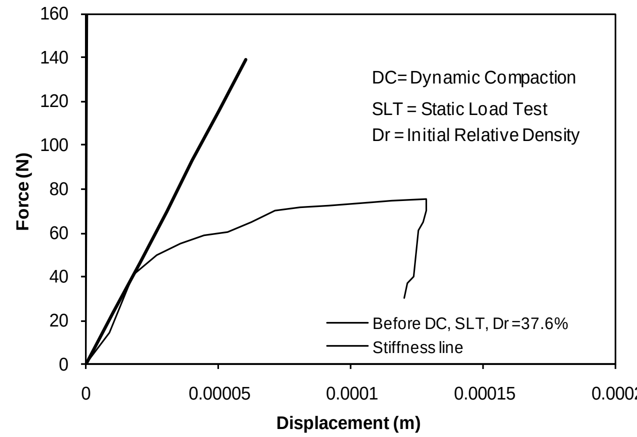

Figure 13. Load-settlement curve (SLT).

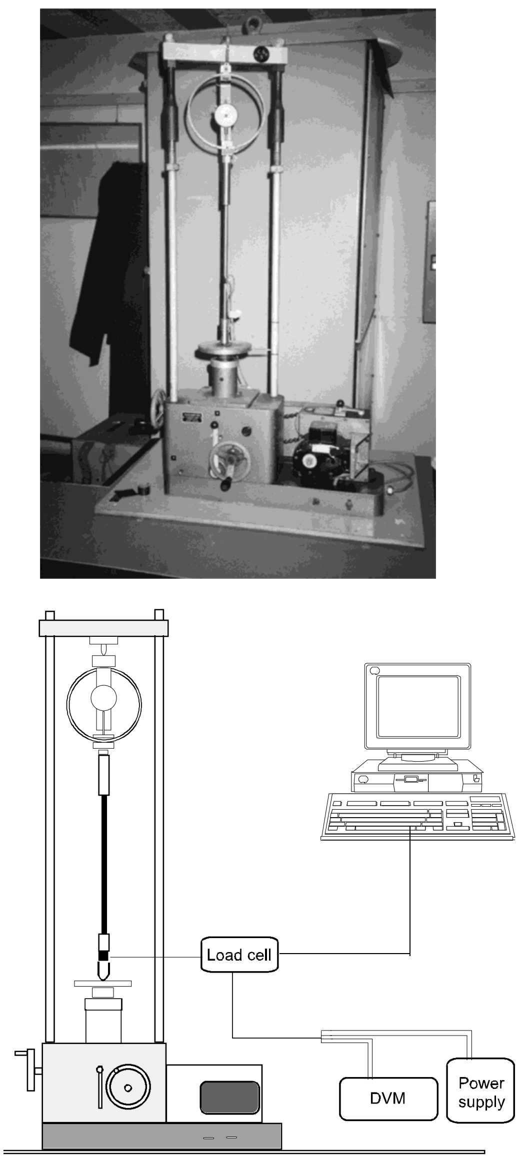

Figure 12. Static load cell calibration equipment.

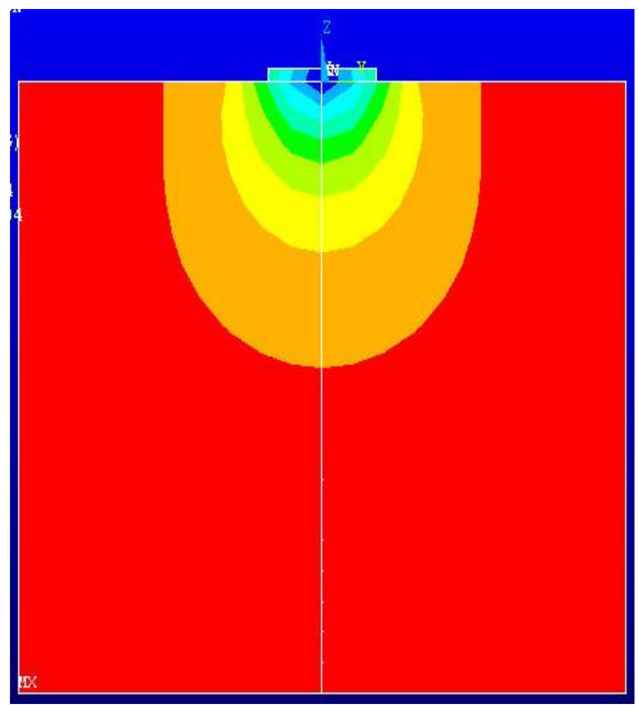

Figure 14. Contours of typical displacement due to monotonic loading (load step F = 10 N, displacement = 7.5 E-6 m).

are preferred by researchers due to reasons such as their low economical costs and more timely delivery of results without necessitating complex experimental procedures and machinery. More specifically, conducting centrifuge experiments for dynamic compaction processes is particularly time consuming and highly laborious where each experiment can take up to two weeks and require three researchers working together. In such a setting, devising reliable numerical methods can be highly beneficial.

The present study demonstrates numerical methods that can be used as low cost and accurate methods for

Table 2. Soil stiffness by experimental static load tests before and after dynamic processes.

Test	Initial relative density Dr (%)	Soil stiffness before dynamic compaction (MN/m)	Soil stiffness after dynamic compaction (MN/m)
1	37.6	1.124	2.154
2	33.5	1.003	2.083
3	35.2	1.072	2.127

Table 3. Soil stiffness by numerical static load tests before and after dynamic processes.

Test	Initial relative density Dr (%)	Soil stiffness before DC(MN/m)	Soil stiffness after DC(MN/m)
1	37.6	1.191	2.062
2	33.5	1.064	1.971
3	35.2	1.135	1.995

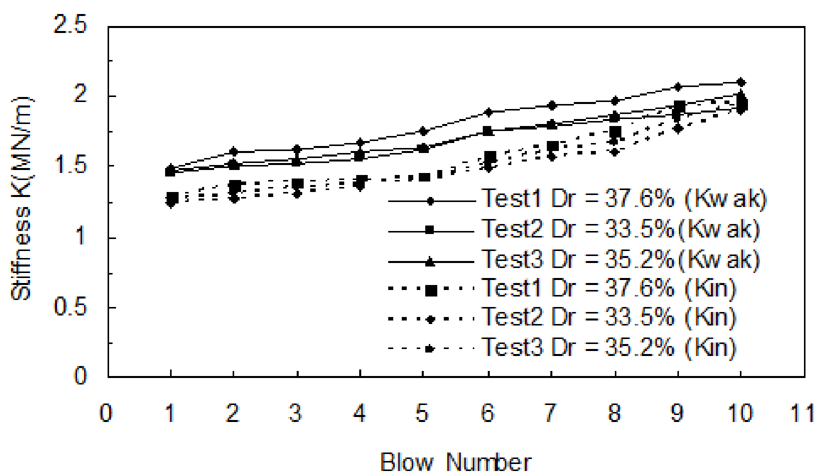

Figure 15. Soil stiffness obtained by WAK Test and initial part of transfer function for Test 1, Test 2 and Test 3.

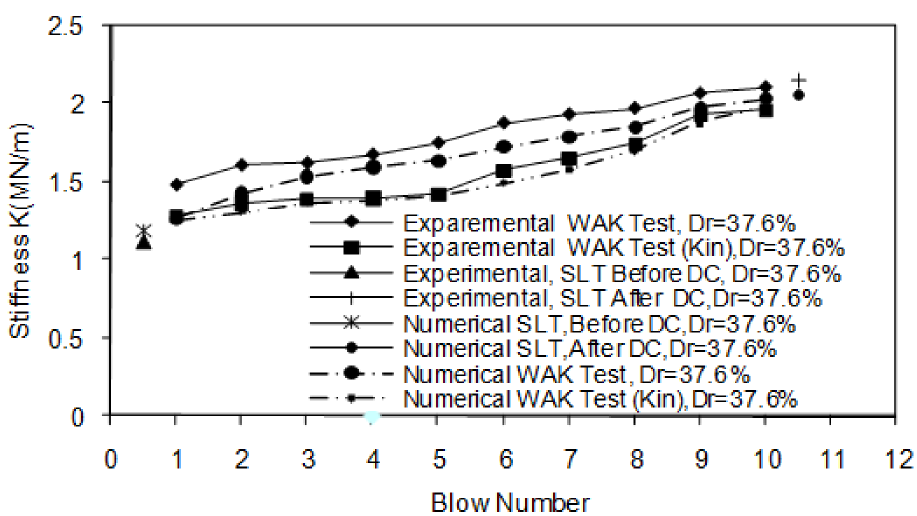

Figure 16. Soil stiffness derived by different methods for Test 1

obtaining sandy soil stiffness. This study can now be extended through development of a numerical model test in flight (multi- g) in the centrifuge to validate soil stiffness computed by the WAK test.

ACKNOWLEDGEMENTS

The support of the University of Yasouj of Iran and the University of Manchester are acknowledged.

REFERENCES

Allen S (1996). University of Wales, Cardiff, U.K.
Allen S, Davies MCR, Brandon JA (1994). In The 19th International Seminar on Modal AnalysisLeuven, Belgium, pp. 935-946.
Briaud JL, Lepert L (1990). WAK test to find spread footing stiffness. ASCE, 116(3): 415-432.
Brooke D, Wynne RJ (1988). Signal processing: principles and applications, Edward Arnold, London.
Charles JA, Watts KS (1982). A field study of the use of the dynamic consolidation ground treatment technique on the soft alluvial soil. Ground Eng., 15(5): 17-25.
Chow YK, Yong DM, Yong KY, Lee SL (1992). Dynamic compaction analysis. ASCE J. Geotech. Eng., 118(8): 1141-1157.
Chow YK, Yong DM, Yong KY, Lee SL (1994). Dynamic compaction of loose granular soils: effect of print spacing. ASCE J. Geotech. Eng., 120(7): 1115-1133.
Clough RW, Penzien J (1975). Dynamic structures, McGraw-Hill, New York.
Gobert AT, Pak RYS (1994). In Centrifuge 94 (ISBN: 9789054103523) (Ed, Leung CF) Rotterdam, Balkema, pp. 277-282.
Lukas RG (1980). Densification of loose deposits by pounding. ASCE J Geotech Eng., 106(GT4): 435-446.
Lukas RG (1995). US Department of Transportation (Technical Report: FHWA-SA-95-037), Federal Highway Administration, Office of Engineering, Office of Technology Applications, Washington..
Lysmer J, Richart FE (1966). Dynamic response of footing to vertical loading. ASCE J Soil Mech Found Div, 92(SM1): 65-91.
Maxwell J, Briaud JL (1983). Texas A & M University, U.S.
Menard L, Broise Y (1975). Theoretical and practical aspects of dynamic consolidation. Geotechnique, 25(1): 3-18.
Merrifield CM, Cruickshank M, Parvizi M (1998). In The International Conference on Geotechnical Centrifuge ModellingTokyo, Japan, pp. 819-824.
Parvizi M (1999). Ph.D. University of Manchester, Manchester.
Parvizi M (2006). In The 5th International Conference on Mechanics and Materials in Design (M2D2006) Porto, Portugal, pp. 1-5.
Parvizi M (2009). Soil response to surface impact loads during low energy dynamic compaction. J. Appl. Sci., 9(11): 2088-2096.
Parvizi M, Merrifield CM (2000). Mechanical behaviour of a sand bed subjected to low energy dynamic compaction. J. Phy. IV., 10(9): 131-135.
Parvizi M, Merrifield CM (2002). In The International Conference on Physical Modelling in Geotechnics (ICPMG'02) Newfoundland, Canada, pp. 400-405.
Parvizi M, Merrifield CM (2004). Centrifuge validation of soil improvement prediction using the WAK test analysis. Ground Improvement, 8(1): 33-37.
Rao SS (1990). Mechanical vibrations (2nd Edition), Addison-Wesley Publishing, Reading.
Tschirart AR, Briaud JL (1992). Texas A & M University, U.S.
Watts KS, Charles JA (1993). In The Conference on Engineering Fills, Newcastle, U.K, pp. 399-412.